NASA TECHNICAL TRANSLATION NASA TT F-15,882

AN IMPLICIT SYSTEM FOR CALCULATION OF FLOW OF A VISCOUS, HEAT-CONDUCTING GAS

Yu.A. Berezin, V.M. Kovenya, and N.N. Yanenko

Translation of "Ob odnoy neyavnoy skheme rascheta techeniya vyazkogo teploprovodnogo gaza," Chislennyye Metody Mekhaniki Sploshnoy Sredy [Numerical methods of mechanics of a continuum], Vol. 3, No. 4, 1972, pp. 3-18

(NASA-TT-F-15882) AN IMPLICIT SYSTEM FOR CALCULATION OF FLOW OF A VISCOUS, HEAT-CONDUCTING GAS (Kanner (Leo) Associates)

N74-31763

CSCL 20D

Unclas

G3/12 47765

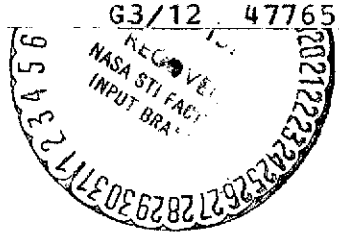

Reproduced by
NATIONAL TECHNICAL
INFORMATION SERVICE
US Department of Commerce
Springfield, VA. 22151

NATIONAL AERONAUTICS AND SPACE ADMINISTRATION
WASHINGTON, D.C. 20546 AUGUST 1974

20

STANDARD TITLE PAGE

1. Report No. NASA TT F-15,882	2. Government Accession No.	3. Recipient's Catalog No.
4. Title and Subtitle AN IMPLICIT SYSTEM FOR CALCULATION OF FLOW OF A VISCOUS, HEAT-CONDUCTING GAS		5. Report Date August 1974 6. Performing Organization Code
7. Author(s) Yu.A. Berezin, V.M. Kovenya, and N.N. Yanenko, Computation Center, Siberian Sector, USSR Acad. of Sci., Novosibirsk		8. Performing Organization Report No. 10. Work Unit No.
9. Performing Organization Name and Address Leo Kanner Associates, P.O. Box 5187 Redwood City, California 94063		11. Contract or Grant No. NASw-2481 13. Type of Report and Period Covered Translation
12. Sponsoring Agency Name and Address NATIONAL AERONAUTICS AND SPACE ADMINISTRATION, WASHINGTON, D.C. 20546		14. Sponsoring Agency Code

15. Supplementary Notes

Translation of "Ob odnoy neyavnoy skheme rascheta techeniya vyazkogo teploprovodnogo gaza," Chislennyye Metody Mekhaniki Sploshnoy Sredy [Numerical methods of mechanics of a continuum], Vol. 3, No. 4, 1972, pp. 3-18.

16. Abstract

An implicit difference scheme of separation of first order accuracy by three-dimensional variables having total approximation, is constructed for a system of equations describing plane flow of a viscous, compressible, heat-conducting gas. Absolute stability of the scheme was demonstrated by the Fourier method and calculations showed that the scheme is stable at least up to Kurant number K = 10. Data and curves are presented on calculations in a steady flow around a wedge and a plate at various angles of attack, Mach and Reynolds numbers, taking account of the associated shock wave, vortex zone and rarefaction zone.

PRICES SUBJECT TO CHANGE

17. Key Words (Selected by Author(s))	18. Distribution Statement
	Unclassified - Unlimited

19. Security Classif. (of this report)	20. Security Classif. (of this page)	21. No. of Pages	22. Price
Unclassified	Unclassified		

AN IMPLICIT SYSTEM FOR CALCULATION OF FLOW OF A VISCOUS, HEAT-CONDUCTING GAS

Yu.A. Berezin, V.M. Kovenya, and N.N. Yanenko
Computation Center, Siberian Sector, USSR Academy of Sciences, Novosibirsk

A sufficiently detailed study of the problem of supersonic /3* flow around a body must be based on use of a complete system of equations of a viscous, compressible, heat-conducting gas. In view of the complexity of these equations, it is impossible to obtain analytical results at the present time, which leads to the necessity for use of numerical methods, which have been worked out intensively over a number of years [1-10].

The explicit schemes examined in [1, 2, 4-6] possess arbitrary stability and, there are severe limitations for them on time spacing τ (or the iteration parameter, in the case of equilibrium problems), at medium and small Reynolds numbers. The scheme presented in [7] removes the limitation on spacing τ, connected with viscosity, but the limitations connected with the normal Kurant condition for gas dynamics without viscosity remain. In this sense, the scheme is intermediate between explicit and implicit ones.

In solution of equilibrium problems, it is important to have an absolutely stable scheme, free of limitations on the iteration parameter. One possible implicit, absolutely stable scheme of the first order of accuracy, with complete approximation, is constructed in our work.

1. Formulation of the Problem /4

A system of equations describing the flow of a viscous, compressible, heat-conducting gas has the following form:

*Numbers in the margin indicate pagination in the foreign text.

$$\frac{\partial \vec{F}}{\partial t} + (\Omega + A)\vec{F} = 0, \qquad (1)$$

where $\Omega = \sum_{i=1}^{4} \Omega_i$ is the differential matrix operator

$$\Omega_1 = \begin{bmatrix} u\frac{\partial}{\partial x} & 0 & 0 & 0 \\ 0 & u\frac{\partial}{\partial x} - \frac{4}{3Re\rho}\frac{\partial}{\partial x}\mu\frac{\partial}{\partial x} & 0 & 0 \\ 0 & 0 & u\frac{\partial}{\partial x} - \frac{1}{Re\rho}\frac{\partial}{\partial x}\mu\frac{\partial}{\partial x} & 0 \\ 0 & 0 & 0 & u\frac{\partial}{\partial x} - \frac{\gamma}{Pr\,Re\rho}\frac{\partial}{\partial x}\mu\frac{\partial}{\partial x} \end{bmatrix};$$

$$\Omega_2 = \begin{bmatrix} v\frac{\partial}{\partial y} & 0 & 0 & 0 \\ 0 & v\frac{\partial}{\partial y} - \frac{1}{Re\rho}\frac{\partial}{\partial y}\mu\frac{\partial}{\partial y} & 0 & 0 \\ 0 & 0 & v\frac{\partial}{\partial y} - \frac{4}{3Re\rho}\frac{\partial}{\partial y}\mu\frac{\partial}{\partial y} & 0 \\ 0 & 0 & 0 & v\frac{\partial}{\partial y} - \frac{\gamma}{Re\,Pr\rho}\frac{\partial}{\partial y}\mu\frac{\partial}{\partial y} \end{bmatrix};$$

$$\Omega_3 = \begin{bmatrix} 0 & \rho\frac{\partial}{\partial x} & 0 & 0 \\ (\gamma-1)\frac{\varepsilon}{\rho}\frac{\partial}{\partial x} & 0 & 0 & (\gamma-1)\frac{\partial}{\partial x} \\ 0 & 0 & 0 & 0 \\ 0 & (\gamma-1)\varepsilon\frac{\partial}{\partial x} & 0 & 0 \end{bmatrix}; \quad \Omega_4 = \begin{bmatrix} 0 & 0 & \rho\frac{\partial}{\partial y} & 0 \\ 0 & 0 & 0 & 0 \\ (\gamma-1)\frac{\varepsilon}{\rho}\frac{\partial}{\partial y} & 0 & 0 & (\gamma-1)\frac{\partial}{\partial y} \\ 0 & 0 & (\gamma-1)\varepsilon\frac{\partial}{\partial y} & 0 \end{bmatrix};$$

$$\vec{F} = \begin{bmatrix} \rho \\ u \\ v \\ \varepsilon \end{bmatrix}; \quad A = -\frac{1}{Re\rho}\begin{bmatrix} 0 & 0 & 0 & 0 \\ 0 & 0 & \varphi_1 & 0 \\ 0 & \varphi_2 & 0 & 0 \\ 0 & \varphi_3 & \varphi_4 & 0 \end{bmatrix};$$

$$\varphi_1 = \frac{\partial}{\partial y}\mu\frac{\partial}{\partial x} - \frac{2}{3}\frac{\partial}{\partial x}\mu\frac{\partial}{\partial y}; \qquad \varphi_2 = \frac{\partial}{\partial x}\mu\frac{\partial}{\partial y} - \frac{2}{3}\frac{\partial}{\partial y}\mu\frac{\partial}{\partial x};$$

$$\varphi_3 = \frac{2}{3}\left(2\frac{\partial u}{\partial x} - \frac{\partial v}{\partial y}\right)\mu\frac{\partial}{\partial x} + \mu\left(\frac{\partial u}{\partial y} + \frac{\partial v}{\partial x}\right)\frac{\partial}{\partial y};$$

$$\varphi_4 = \frac{2}{3}\left(2\frac{\partial v}{\partial y} - \frac{\partial u}{\partial x}\right)\mu\frac{\partial}{\partial y} + \mu\left(\frac{\partial u}{\partial y} + \frac{\partial v}{\partial x}\right)\frac{\partial}{\partial x};$$

The following designations were used here: x, y are the cartesian coordinates; t is time; u, v are the projections of the velocity vector on the x, y axes; ρ, ε are the density and internal energy; μ is the coefficient of dynamic viscosity, $\gamma = C_p/C_v$ is the ratio of the heat capacity; Pr is the Prandtl number; Re is the Reynolds number. System (1)-(3) is written in dimensionless variables: /5

$$t=\frac{u_0\bar{t}}{L};\ x=\frac{\bar{x}}{L},\ y=\frac{\bar{y}}{L},\ u=\frac{\bar{u}}{u_0},\ v=\frac{\bar{v}}{u_0},\ \varepsilon=\frac{\bar{\varepsilon}}{u_0^2},\ \rho=\bar{\rho}/\rho_0,$$
$$\mu=\bar{\mu}/\mu_0,\quad Pr=\frac{c_p\mu_0}{\lambda_0},\quad Re=\frac{\rho_0 u_0 L}{\mu_0}$$

(the dashes concern dimensional quantities and subscript 0, to values in the incoming flow]; λ_0 are the heat conductivity coefficients, L is the length of the body, u_0 is the speed of the incoming flow.

The gas pressure p is excluded from systems (1)-(3), by means of the equation of state $p = (\gamma - 1)\rho\varepsilon$. It is assumed that the coefficients of viscosity μ and heat conductivity λ are exponential functions of the internal energy (C_p, C_v = const).

Conditions of adhesion and heat insulation are placed on the surface of the body:

$$\left.\begin{aligned} &u=v=0;\\ &\frac{\partial\varepsilon}{\partial n}=0. \end{aligned}\right| \qquad (4)$$

To find the stationary solution of the problem of flow-around

$$(\Omega+A)\bar{F}=0, \qquad (5)$$

the steady state establishment method is used.

2. Difference Scheme

We introduce into cylinder $D_H = D \times H$ (D is the rectangular region, in which a numerical solution is sought, H = [0, T] $\Gamma = G \times H$ is the boundary) a difference grid with coefficients:

$$t=\tau\times n;\ x_i=\sum_{i=0}^{i}h_1(i);\quad y_k=\sum_{k_1}^{k}h_2(k),\ n=0,\dots,N.$$

Here, τ is the iteration parameter, $h_1(t)$ and $h_2(k)$ are the grid spacings on the x and y coordinates. We introduce the network function $\vec{F}_h^n(\rho_{i,k}^n, u_{i,k}^n, v_{i,k}^n, \xi_{i,k}^n)$ and difference operators Ω^{h_j}, A^h, approximating the initial differential matrix operators, with /6 first or second order accuracy. The difference operator of the boundary conditions l^h approximates (4), with second order accuracy. In accordance with differential problem (4), (5), we set up the difference problem:

in cylinder D_H, to find the solution of equation

$$(\Omega^h + A^h)\vec{F}_h = 0, \tag{6}$$

with boundary conditions

$$l^h \vec{F}_h = 0. \tag{7}$$

For solution of difference problem (6) by the establishment method, the following implicit separation scheme is assumed:

$$\begin{aligned}
&(E+\tau_1\Omega_1^h)\vec{E}^{n+1/4} = -\tau(\Omega^h + A^h)\vec{F}_h^n,\\
&(E+\tau_2\Omega_2^h)\vec{E}^{n+2/4} = \vec{E}^{n+1/4},\\
&(E+\tau_3\Omega_3^h)\vec{E}^{n+3/4} = \vec{E}^{n+2/4},\\
&(E+\tau_4\Omega_4^h)\vec{E}^{n+1} = \vec{E}^{n+3/4},\\
&\vec{F}^{n+1} = \vec{F}^n + \vec{E}^{n+1},
\end{aligned} \tag{8}$$

where $\vec{E}^{n+j/4}$ $(j=1,2,3,4)$ is an auxiliary vector.

Elimination of fractional steps gives a universal algorithm scheme [11], having the property of complete approximation:

$$\begin{aligned}
&B\frac{\vec{F}^{n+1} - \vec{F}^n}{\tau} = -(\Omega^h + A^h)\vec{F}_h^n\\
&B = \prod_{j=1}^{4}(E+\tau_j\Omega_j^h);\ \Omega^h = \sum_{j=1}^{4}\Omega_j^h.
\end{aligned} \tag{9}$$

Difference scheme (8) permits laborious matrix trials to be avoided. A similar separation scheme, but not having complete

approximation, was examined in [12].

We examine the stability of a linearized scheme corresponding to scheme (9), by the Fourier method, at $\tau_j = \tau$. Selecting the solution in the form we obtain the following characteristic equation: /7

$$[t_0(\lambda-1)+\omega_0][t_1(\lambda-1)+\omega_1]^2[t_2(\lambda-1)+\omega_2]+(\gamma-1)\varepsilon\{[t_1(\lambda-1)+1]\{[t_0(\lambda-1)+\omega_0][t_2(\lambda-1)+1](\gamma-1)+[t_0(\lambda-1)+1][t_2(\lambda-1)+\omega_0]\}\{(\gamma-1)\varepsilon d_1^2 d_2^2 t(\lambda-1)+(d_1^2+d_2^2)[t_1(\lambda-1)+\omega_1]\}\}=0, \quad (10)$$

where

$$\omega_0=a+b;\ \omega_1=\omega_0+r_1+r_2;\quad \omega_2=\omega_0+\delta(r_1+r_2);$$
$$t_0=(1+a)(1+b);\quad t_1=(1+a+r_1)(1+b+r_2);$$
$$t_2=(1+a+\delta r_1)(1+b+\delta r_2);\quad d_1=i\frac{\tau}{h_1}\sin jh_1;\quad d_2=i\frac{\tau}{h_2}\sin \kappa h_2;$$
$$r_1=\frac{4\mu\tau}{Re\rho h_1^2}\sin^2\frac{jh_1}{2};\qquad r_2=\frac{4\mu\tau}{Re\rho h_2^2}\sin^2\frac{\kappa h_2}{2};$$
$$a=2\frac{\tau}{h_1}|u|\sin^2\frac{jh_1}{2}+i\frac{\tau}{h_1}u\cos jh_1;$$
$$b=2\frac{\tau}{h_2}|v|\sin^2\frac{\kappa h_2}{2}+i\frac{\tau}{h_2}v\cos\kappa h_2;$$

At sufficiently large values of internal energy ε, which corresponds to regions behind strong shock waves (in hypersonic flows), Eq. (10) takes the form:

$$[t_1(\lambda-1)+1]\{[t_0(\lambda-1)+\omega_0][t_2(\lambda-1)+1](\gamma-1)+[t_0(\lambda-1)+1][t_2(\lambda-1)+\omega_2]\}(\lambda-1)=0. \quad (10a)$$

In the absence of viscosity ($r_1 = 0$), the root of (10a) equals:

$$\lambda_1=1;\quad \lambda_{2,3}=1-\frac{1}{t_0};\quad \lambda_4=1-\frac{\omega_0}{t_0}, \quad (11)$$

and, in the case of low velocities $\lambda_1=1;\ \lambda_2=1-\frac{1}{t_2};$

$$\lambda_{3,4}=\frac{(2\tau-1)t_2-\omega_2-(\tau-1)\pm\sqrt{(t_2+\omega_2+(\tau-1))^2-4\tau\omega_2 t_2}}{2\tau t_2} \qquad (12)$$

At small values of the internal energy ε (regions of high rarefaction), the characteristic equation

$$[t_0(\lambda-1)+\omega_0][t_1(\lambda-1)+\omega_1]^2[t_2(\lambda-1)+\omega_2]=0 \qquad (8)$$

has the roots

$$\lambda_1=1-\frac{\omega_0}{t_0};\quad \lambda_{2,3}=1-\frac{\omega_1}{t_1};\quad \lambda_4=1-\frac{\omega_2}{t_2}; \qquad (13)$$

It follows from formulas (11)-(13) that $\lambda = \max|\lambda_i| \leq 1$, i.e., there is absolute stability in the limiting cases of scheme (9) examined. It can be expected that, in the general case, the scheme will be stable. Of course, the linear analysis carried out is not sufficient; therefore, a test is necessary, by means of systematic calculations. Such a test was carried out, and it turned out that the scheme is stable, at least up to Kurant number $K \leq 10$, where

$$K=\frac{\tau}{h_1 h_2}(h_1|v|+h_2|u|+c\cdot\max(h_1,h_2)).$$

The proposed difference scheme can be used for calculation of axisymmetric flows.

3. Examples of Numerical Calculations

1) Flow around a wedge. Calculations were carried out of a plane flow of a viscous, compressible, heat-conducting gas around a wedge of length L along the x axis, at an arbitrary angle of attack. Conditions (4) were placed on the surface of the body, and the density was determined from the continuity equation, with second order accuracy. Viscosity μ was determined by the formula $\mu = (\varepsilon/\varepsilon_0)^{\omega}$, $\omega = 0.75$.

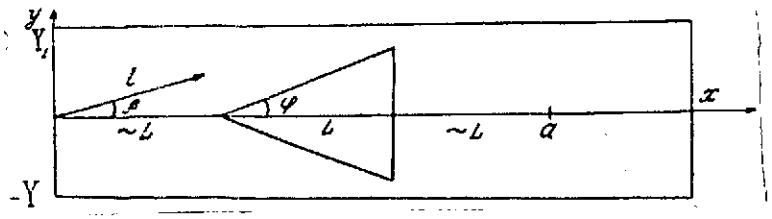

The front, upper and lower boundaries of the calculation region were selected, so that conditions corresponding to unperturbed flow could be placed on them: /9

$$u = u_0 \cos\beta;\ v = -u_0 \sin\beta;\ \rho = 1,\ e = \frac{1}{\gamma(\gamma-1)M^2}, \qquad (14)$$

where β is the angle of attack. It turned out that it is sufficient to select a distance from the wedge to the front boundary of the region on the order of L and, to the upper and lower boundaries, 3-5L. The rear boundary of the region was removed to a distance X - 5-15L from the bottom of the wedge and boundary conditions $\partial f/\partial l = 0$, where l is the direction of the incoming flow, were set on it. Comparison of numerical solutions in section x = 5L, at X = 7L and X = 12L, shows that their difference is not over 1%.

The spacings of the adjusted difference network along the x axis from zero to a were selected to be uniform and equal to $h_i = \Delta h_1 = 1/m$ (m is the number of points on the wedge); at x > a, nonuniform spacing was selected by formula $h_i = h_{i-1} + \Delta h_1$. The spacing along the y axis in the vicinity of the wedge was assigned by the formula $h_K = \Delta h_2 = \Delta h_1 \tan\phi$ and, in the remaining part of the region, by the formula $h_K = h_{K-1} + \Delta h_2$. The calculation region contained 56 y points and 40 x points, i.e., 2360 points in all; the number of points on the body m = 10. As initial data over the entire region, except the boundaries of the body, conditions (14) were assigned. The numerical calculations were carried out at different values of the iteration parameter τ = 0.03, 0.05, 0.1, 0.2 and 0.3, which correspond to Kurant numbers K = 0.5-8.5. Comparison of the steady numerical solutions on the surface of the bodies for different τ and Δh has shown that, with change in τ, coincidence of the values of

the functions sought occurred to the third decimal place (i.e., the steady solution does not depend on τ) and, with a 60% decrease in grid spacing, the differences were not over 5-6%. The establishment criterion was satisfaction of the condition

$$\max\left|\frac{\partial \rho}{\partial t}\right| \leq \delta, \qquad (15)$$

where $\delta = 10^{-3}$ over the entire calculation region.

The results of calculation of flow around a wedge at zero angle of attack, with $\gamma = 1.4$, $Pr = 0.72$, are presented in Table 1 and in Graphs 1-3.

TABLE 1. /10

M	2	2	2	2	3	3	3
Re	100	250	500	1000	100	250	500
$\tan\varphi$	0.3	0.3	0.3	0.3	0.3	0.3	0.3
$\tilde{x}_0$	-	0.36	0.65	0.9	-	0.1	0.36
ϵ	0.606	0.591	0.550	0.482	0.368	0.310	0.264
ρ	0.410	0.476	0.591	0.601	0.273	0.427	0.519

Here, $\tilde{x}_0$ is the rear critical point (boundary of the return flow zone on the axis of symmetry $y = 0$), ϵ and ρ are the internal energy and density at the bottom of the wedge, at $y = 0$ and M, Re are the Mach and Reynolds numbers of an unperturbed flow. The change in $\tilde{x}_0$, as a function of the M and Re numbers, coincides qualitatively with calculations [5].

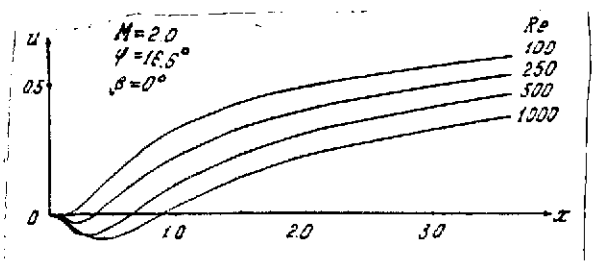

Fig. 1.

The distribution of x, the velocity components on the axis $y = 0$, is given in Fig. 1, at various Re numbers (100-1000), for the case

$M = 2.0$, $\phi = 16.6°$. An increase in Reynolds number leads to an increase in the return flow region. We make an estimate of the calculated viscosity in the track next to the body. The physical viscosity $\nu_\phi = \mu/\mathrm{Re}\rho$ directly beyond the bottom shear, is on the order of ~ 0.02 (at $\rho \approx 0.5$, $\mu \approx 1.5$, $\mathrm{Re} \approx 100$–300), and the calculated, determined by formula $\nu_{cr} \approx \frac{h}{2}|u_i|$, is on the order of ~ 0.001–0.002 ($h_1 = 0.1$, $|u_i| \simeq 0.03$–0.1, $i = 1, 2$). In this manner, the calculated viscosity is considerably less than the physical in the near track.

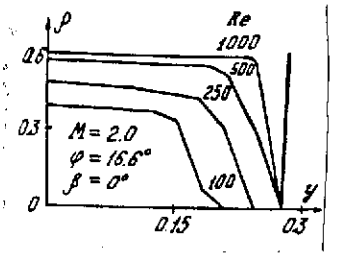

Fig. 2.

Distribution of the gas density at the bottom of the wedge is presented in Fig. 2, at various Re and $M = 2$, $\phi = 16.6°$. At the points closest to the corner, a drop in density takes place, to a value close to zero. With increase in Re, this zone decreased and, at $\mathrm{Re} = 1000$, it degenerated into a single point. This feature of the flow was noted earlier in [5]. A decrease in density is observed along the generatrix of the wedge, from values in the vicinity of the tip close to a normal shock to almost unperturbed values. The internal energy along the generatrix is nearly a constant, which decreases with increase in Re. The curves of the x components of the velocity at various distances from the bottom of the wedge along the axis of symmetry are given in Fig. 3, at $\mathrm{Re} = 1000$, $M = 2$, $\phi = 16.6$. The calculations show that an associated shock wave forms ahead of the wedge (Fig. 4). With increase in Re number (> 250), the velocity distribution in the shock wave is almost unchanged, which apparently can be explained by the effect of the calculated viscosity. For a more detailed explanation of the nature of the flow in the vicinity of the tip, calculations, according to schemes of a high order of accuracy, are necessary.

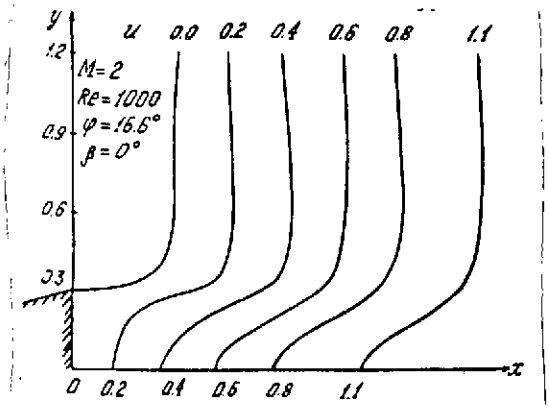

Fig. 3.

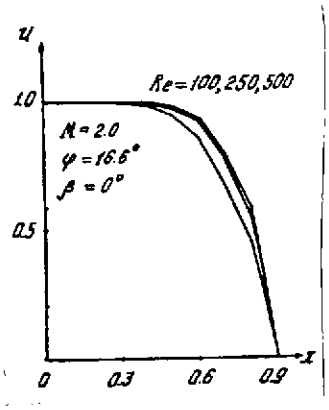

Fig. 4.

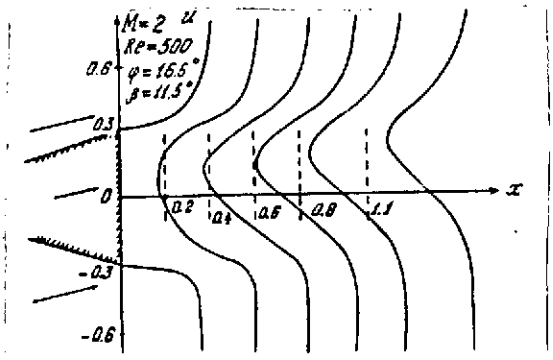

Fig. 5.

Calculations of flow around a wedge at a nonzero angle of attack were carried out (β = 11.5°; M = 2-3; Re = 100, 500, 1000; ϕ = 16.6°, 29°). Curves of the distribution of internal energy and of the x component of the velocity at various distances from the wedge are presented in Figs. 5 and 6 (M = 2, Re = = 500, ϕ = 16.6°). It is evident from Fig. 5 that the vortex axis is located along the direction of the incoming flow. As is well-known (see, for example, [13]), there is a fan of rarefaction waves beyond the body around which the flow takes place. A zone of reduced internal energy is seen well in Fig. 6, which corresponds to these rarefaction waves. A similar phenomenon was noted in our calculations of flow around a wedge at a zero angle of attack. /12

2) Flow around a plate. Calculations were carried out of flow around a plate, of length L = 1 and thickness $\delta = \Delta h_2$, at various angles of attack. The calculation region and grid spacing were selected just as in the case of the wedge. /13

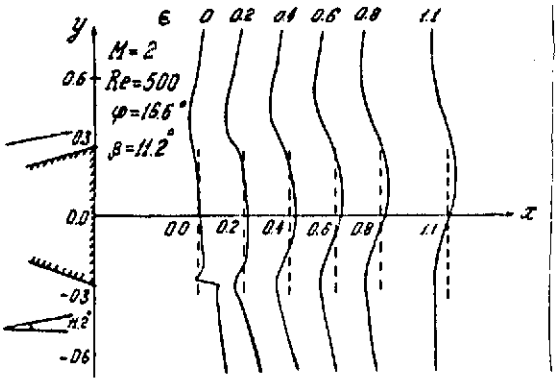

Fig. 6.

Typical calculations were carried out at $\tau = 0.1$–0.2, $\Delta h_1 = 0.1$ and $\Delta h_2 = 0.03$. To accelerate the convergence, the steady solution at smaller Reynolds numbers was taken as the initial conditions, which led to approximately a 30% decrease in number of iterations. The flow was considered to be steady upon satisfying conditions (15). The parameters of the calculated versions are presented in Table 2.

TABLE 2.

M	2	2	2	2	2	3	3	3
Re	100	200	400	500	1000	100	200	400
Angle of attack in °	0	0	0	0	0	0	0	0

5	5	10	2	2	3	2	2	2
200	400	200	400	1000	200	400	2000	4000
0	0	0	23	23	11.5	34.5	23	23

In calculations of flow around a plate at a zero angle of attack, the formation of a boundary layer was studied, as a function of the Mach and Reynolds numbers. It is known (see, for example [13]), that the thickness of the boundary layer in flow around a body by an incompressible fluid is determined by the formula $\delta \sim Re^{-1/2}$, with a proportionality coefficient on the order of unity. In the case of a compressible gas, as the calculations show, a qualitative dependence of thickness δ on Reynolds number is preserved (Fig. 7), but the value of δ is greater; this increase in thickness δ is determined by the interaction of the thermal and boundary layers [13]. A

characteristic feature of the flow is thickening of the boundary layer on the front part of the plate, where fusion of it with the associated shock wave takes place. The increase in boundary layer thickness with increase in Mach number noted in [13] /14 attracts attention (Fig. 8).

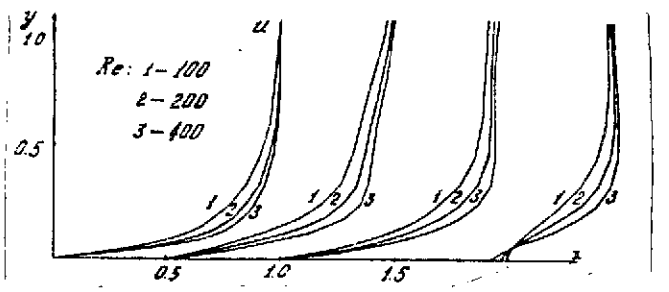

Fig. 7.

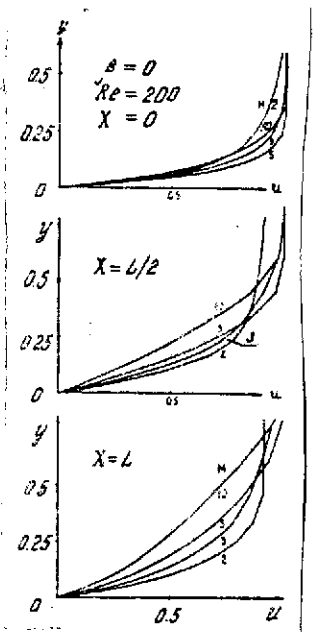

Fig. 8.

At M = 10, the velocity profile in the zone of the developed boundary layer is close to linear. Distribution of density on the plate depends slightly on Re number. A decrease in density is observed along the plate, to values less than in unperturbed flow ($\rho \approx 0.75\rho_0$, M = 2). In the front section of the plate, a sharp increase in density is observed, which is connected with shock wave formation. The distribution of internal energy along the plate is almost linear; there is a discontinuity in it, connected with increase in entropy in the transition through the shock wave (the so-called entropy layer), only in the vicinity of the origin of the plate. The increase in internal energy in the plate over the energy in the incoming flow is small, and it decreases with increase in Reynolds number.

The local and total resistance factors of the plate were computed in the calculations, by the following formulas:

$$c_f = \frac{\mu}{Re}\left.\frac{\partial u}{\partial y}\right|_{y=0}, \qquad c_f = \frac{2}{Re_0}\int_0^L \mu \left.\frac{\partial u}{\partial y}\right|_{y=0} dx. \tag{16}$$

/15

A comparison of the coefficients of frictional resistance of the plate, calculated by formula (16) and by the empirical formula of Junge [13] is made in Table 3:

$$c_f = \frac{1}{\sqrt{Re_x}} \cdot 0.664\left[1 + 0.365(\gamma-1)M_\infty^2\sqrt{Pr}\right]^{\frac{\omega-1}{2}}, \qquad c_f = \frac{2}{0}\int_0^L c_f\, dx. \tag{17}$$

The increase in divergence of the calculated resistance factor from that determined by formula (17) can be explained by the fact that formula (17) holds true for a boundary layer, not distorted by the effect of the shock wave. In our calculations, there always is an interaction of the boundary layer with the associated shock wave, which leads to some change in the velocity profile next to the body. Moreover, with increase in Re number, the relative effect of the calculated viscosity increases, leading to errors in calculation of the resistance factor. As in flow around a wedge, there is a curvature of the shock wave in these calculations, in the front part of the plate, because of the viscous interaction. The slope of the shock wave downstream approximates its slope in a nonviscous gas (for M = 2, Re = 500, the shock wave slope angle in a nonviscous gas is ∿30°, but the calculation gives ∿32°).

TABLE 3. RESISTANCE FACTOR OF PLATE (ω =0.75).

M	Re	Calculated Resistance	Theoretical Resistance	$\Delta = (C_f)_c - (C_f)_T$	$\frac{\Delta}{(C_f)_T}$ %
2	100	0.1366	0.1328	0.0038	2.86
2	200	0.0926	0.0940	-0.0014	-1.5
2	400	0.0618	0.0664	-0.0046	-6.93
3	100	0.1401	0.1328	-0.0073	-5.5
3	200	0.0940	0.0940	-0.0036	-3.84
3	400	0.0601	0.0661	-0.0060	-9.05

Calculations also were made of flow around a plate at a nonzero angle of attack. The internal energy and density on the upwind side is considerably greater than on the downwind (Fig. 9). /16 There is a rarefaction zone on the downwind side, in which the velocity x component profiles are close to linear; the stream is displaced in the direction of flow (Fig. 10). At angle of attack β = 0.4, calculations were carried out at Reynolds numbers Re = 1000, 2000 and 4000, M = 2. It was assumed that, at large Re numbers, vortex formation will occur. The calculations showed that, at Re = 1000, a change in s e t . of the velocity arises at one point above the end of the plate; however, further /17 increase in Reynolds number did not lead to the appearance of vortexes. In flow around a plate, stagnant zones do not form; therefore, the velocity of the flow and, of course, the calculated viscosity in the vicinity of the plate is quite high, which apparently can explain the absence of vortexes. A test was made of satisfaction of the laws of conservation of mass and total energy, to check the accuracy of the calculations. The error in conservation of mass was not over 1.5% and of energy, 0.3%.

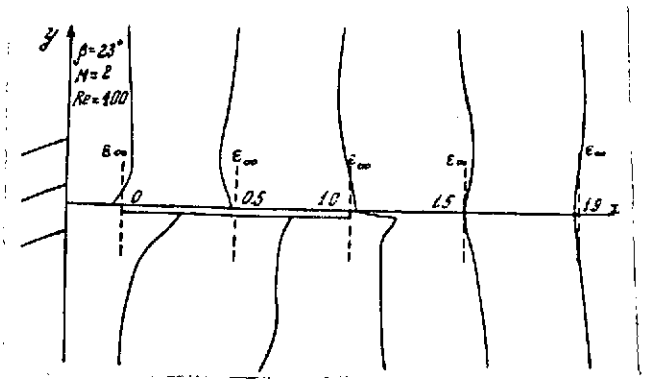

Fig. 9.

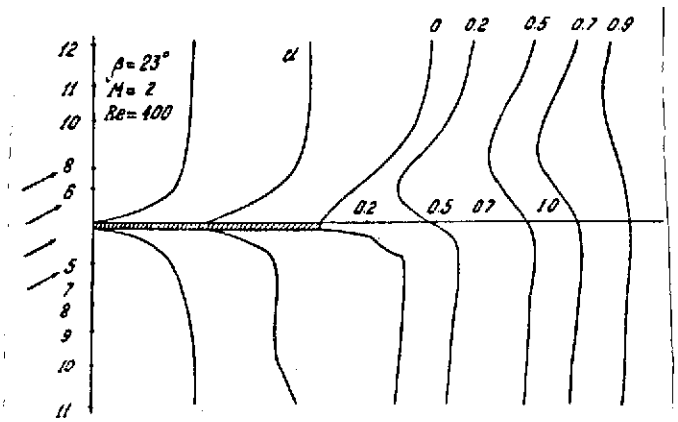

Fig. 10.

In typical calculations, the number of iterations to steady flow is ∿200-250 for the wedge and 150 for the plate, and the time of calculation of one version on the BESM-6 computer is 16-25 minutes.

Conclusions

1. An implicity difference scheme of separation of first order accuracy by directional variables having complete approximation, was constructed for a system of equations describing plane flow of a viscous, compressible, heat-conducting gas.

2. The absolute stability of this scheme in the limiting cases was demonstrated by the Fourier method.

3. Systematic calculations showed that the scheme is stable at least up to Kurant number K = 10.

4. Steady flow up to $\varepsilon = 10^{-3}$ ($\varepsilon = \max\left|\frac{\partial \rho}{\partial t}\right|$) takes place in 150-300 iterations.

5. The scheme permits calculations to be carried out under arbitrarily assigned initial conditions.

6. A picture was obtained of flow around a wedge and a plate at various angles of attack (associated shock wave, vortex zone and rarefaction zone).

REFERENCES

1. Rikhtmayer, R., Raznostnyye metody resheniya krayevykh zadach [Difference methods of solution of boundary problems], Foreign Language Literature Publishing House, 1960.

2. Lax, P.D. and B. Wendroff, "Difference schemes for hyperbolic equations with high order of accuracy," Comm. Pure Appl. Math. 17/3 (1964).

3. Godunov, S.K., A.V. Zabrodin, and G.P. Prokopov, "Difference scheme for two-dimensional nonequilibrium problems of gas dynamics and calculations of flowaround with outgoing shock wave," ZhVM i MF, No. 6 (1961).

4. Brailovskaya, I.Yu., "Difference scheme for numerical solution of two-dimensional, nonequilibrium Navier-Stokes equations for a compressible gas," DAN SSSR 160/5 (1965).

5. Brailovskaya, I.Yu., "Explicit difference methods for calculation of breakaway flows of a viscous, compressible gas," Nekotoryye primeneniya metoda setok v gazovoy dinamike [Some applications of the network method in gas dynamics], Vol. 4, Izd. MGU, 1971.

6. Pavlov, B.M., "Numerical study of supersonic flow around blunt bodies by a viscous gas flow," ibid.

7. Polezhayev, V.I., "Numerical solution of system of two-dimensional, nonequilibrium Navier-Stokes equations for a compressible gas in a closed region," Izv. AN SSSR, ser. mekh. zhidk. i gaza, No. 2 (1967).

8. Lyubimov, A.N. and V.V. Rusanov, Techeniye gaza okolo tupykh tel [Gas flow around blunt bodies], "Nauka" Press, Moscow, 1970.

9. Yanenko, N.N., V.D. Frolov, and V.Ye. Neuvazhayev, "Use of the separation method for numerical calculation of movement of a heat-conducting gas in curvilinear coordinates," Izv. SO AN SSSR, ser. tekhn. nauk 8/2 (1967).

10. Belotserkovskiy, O.M. and Yu.M. Davydov, "The 'large particle' method for gas dynamics problems," Inf. byull. "Chislenniye metody mekhaniki sploshnoy sredy" [Information bulletin: Numerical methods of mechanics of a continuum], Vol. 1, No. 3, 1970.

11. Marchuk, G.I. and N.N. Yanenko, "Use of the separation method (fractional steps) for solution of mathematical physics problems," in the collection Nekotoryye voprosy vychislitel'noy i prikladnoy matematiki [Some problems in computational and applied mathematics], "Nauka" Press, Novosibirsk, 1966.

12. Kovenya, V.M., "Numerical method of calculation of equilibrium Navier-Stokes equations of a compressible gas," Inf. byull. "Chislenniye metody mekhaniki sploshnoy sredy" [Information bulletin: Numerical methods of mechanics of a continuum], Vol. 1, No. 3, 1970.

13. Loytsyanskiy, L.G., Mekhanika zhidkosti i gaza [Fluid and gas mechanics], "Nauka" Press, Moscow, 1970.